Electronic Supplementary Information
for

A chiral Si(IV) complex bearing a 1,2,4-triazole-2,2'-diphenol ligand: synthesis, (chiro-)optical properties and computational investigation

Valerio Giuso,†[a] Thibault Thierry,†[a] Christophe Gourlaouen,[b] Pierluigi Mercandelli,[c] Nicolas Vanthuyne,[d] Matteo Mauro*[a] and Stéphane Bellemin-Laponnaz*[a]

[a] Université de Strasbourg & CNRS, Institut de Physique et Chimie des Matériaux de Strasbourg UMR 7504, F-67034 Strasbourg, France
[b] Laboratoire de Modélisation et Simulation Moléculaire, UMR7140 Chimie de la Matière Complexe, Institut Le Bel, F-67081 Strasbourg, France
[c] Università degli Studi di Milano, Dipartimento di Chimica, 20133 Milan, Italy.
[d] Aix-Marseille Université, CNRS Centrale Marseille, iSm2, 13284 Marseille, France

* Corresponding authors
Email of corresponding authors:
Stéphane Bellemin-Laponnaz: bellemin@unistra.fr
Matteo Mauro: mauro@unistra.fr
ł T.T. and V.G. have equally contributed to this work.

Contents

Supplementary NMR Spectra

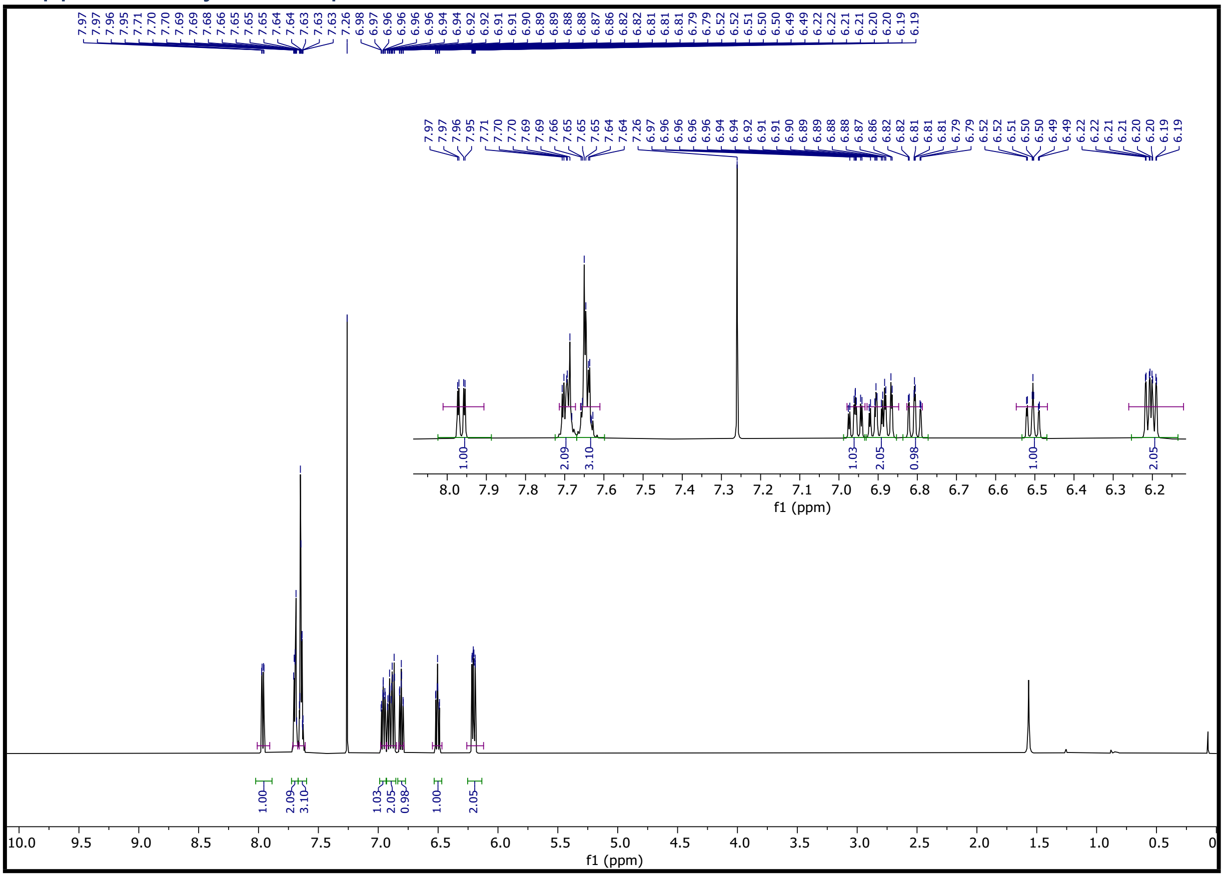

Figure S 1 - [1]H NMR spectrum of **Si(ONO)$_2$** in $CDCl_3$.

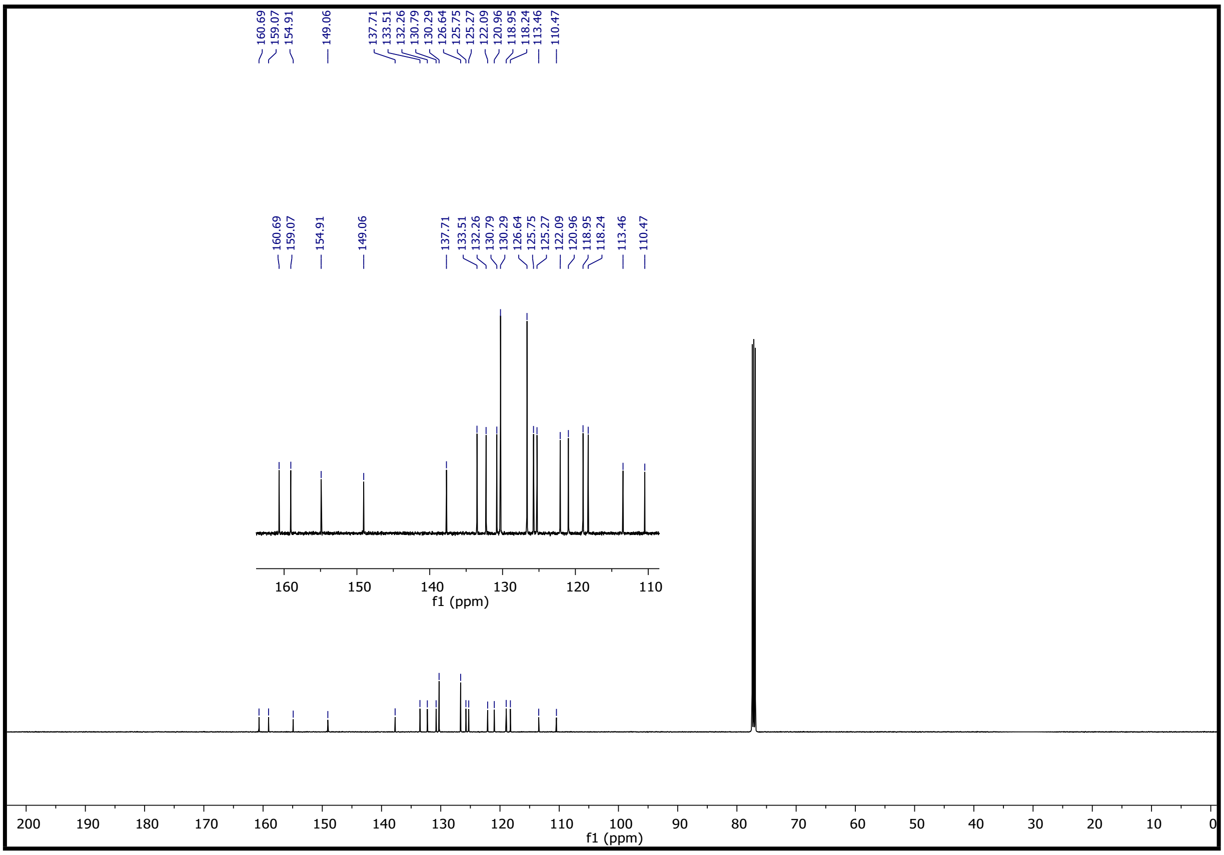

Figure S 2 - $^{13}C\{^{1}H\}$ NMR spectrum of $Si(ONO)_2$ in $CDCl_3$.

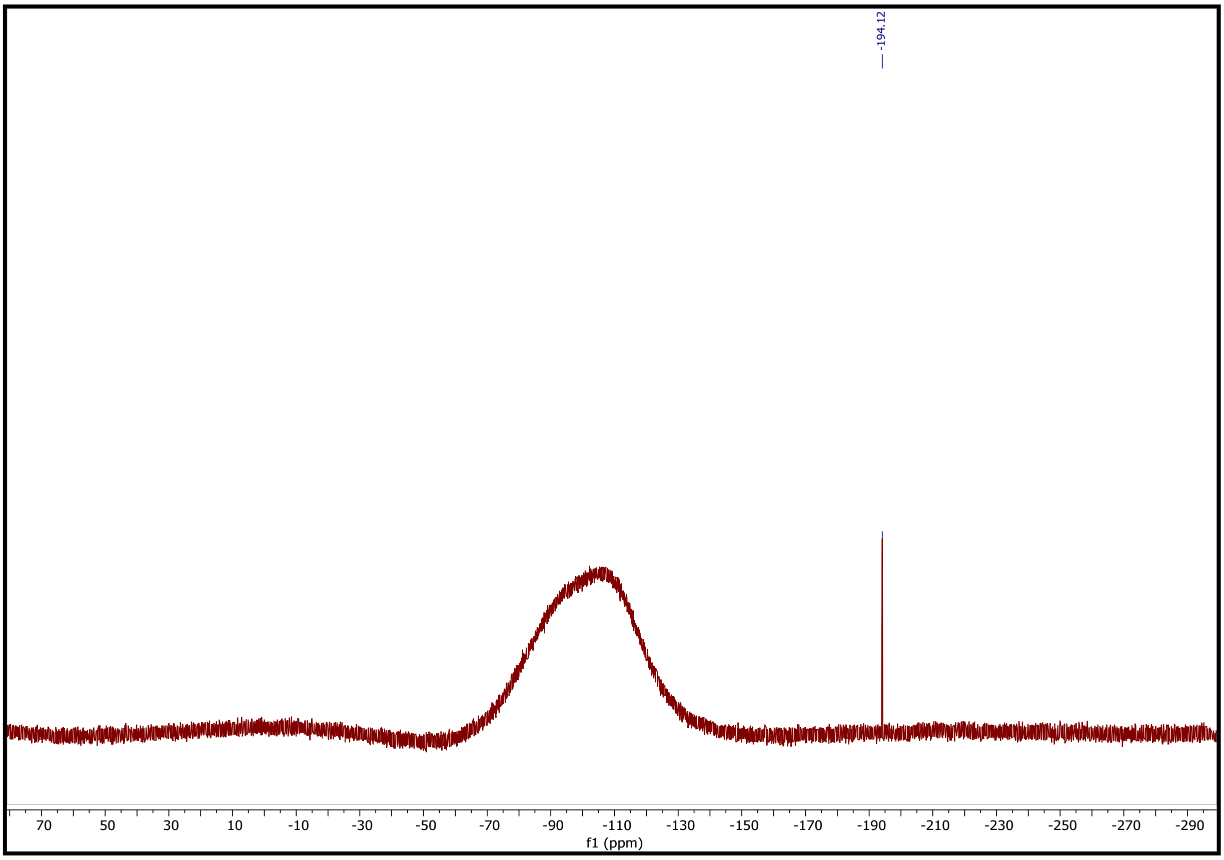

Figure S 3 - ^{29}Si NMR spectrum of $Si(ONO)_2$ in $CDCl_3$.

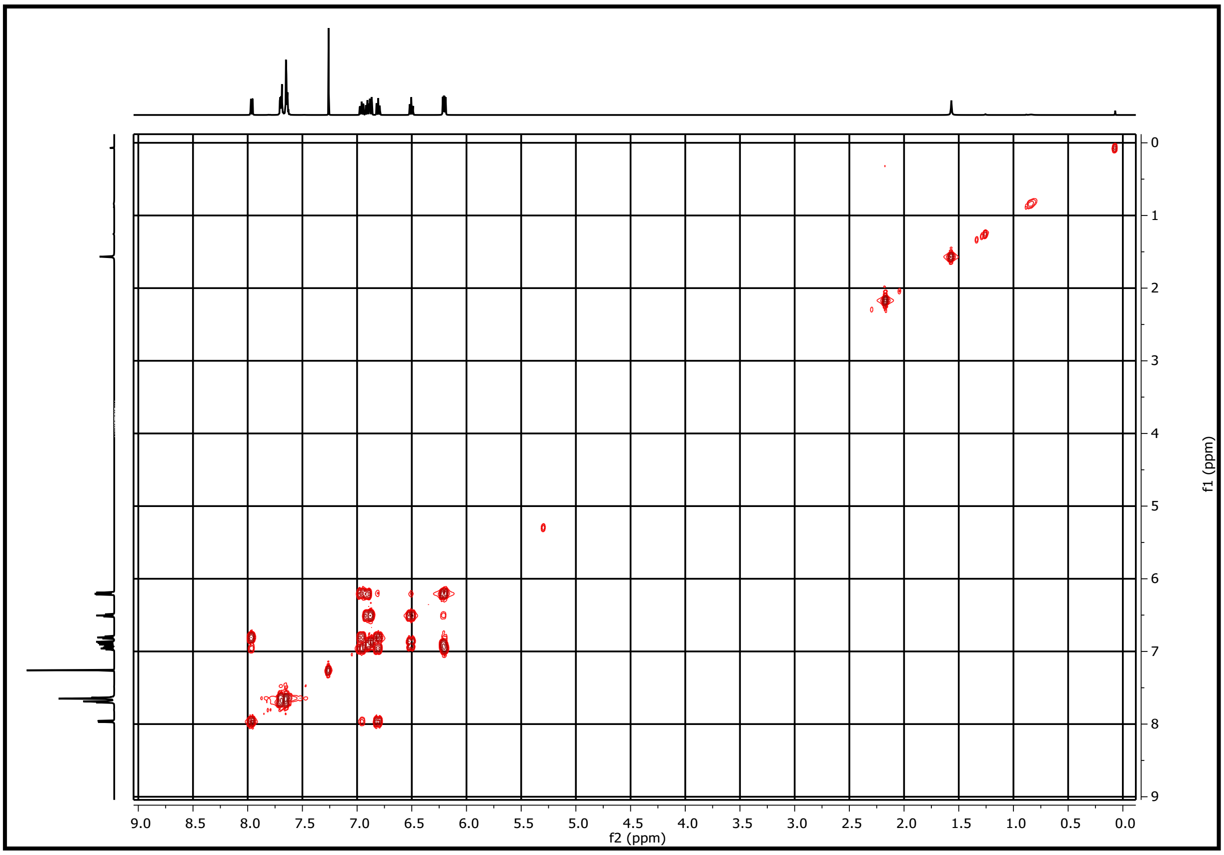

Figure S4. ^{1}H-^{1}H COSY NMR spectrum of $Si(ONO)_2$ in $CDCl_3$

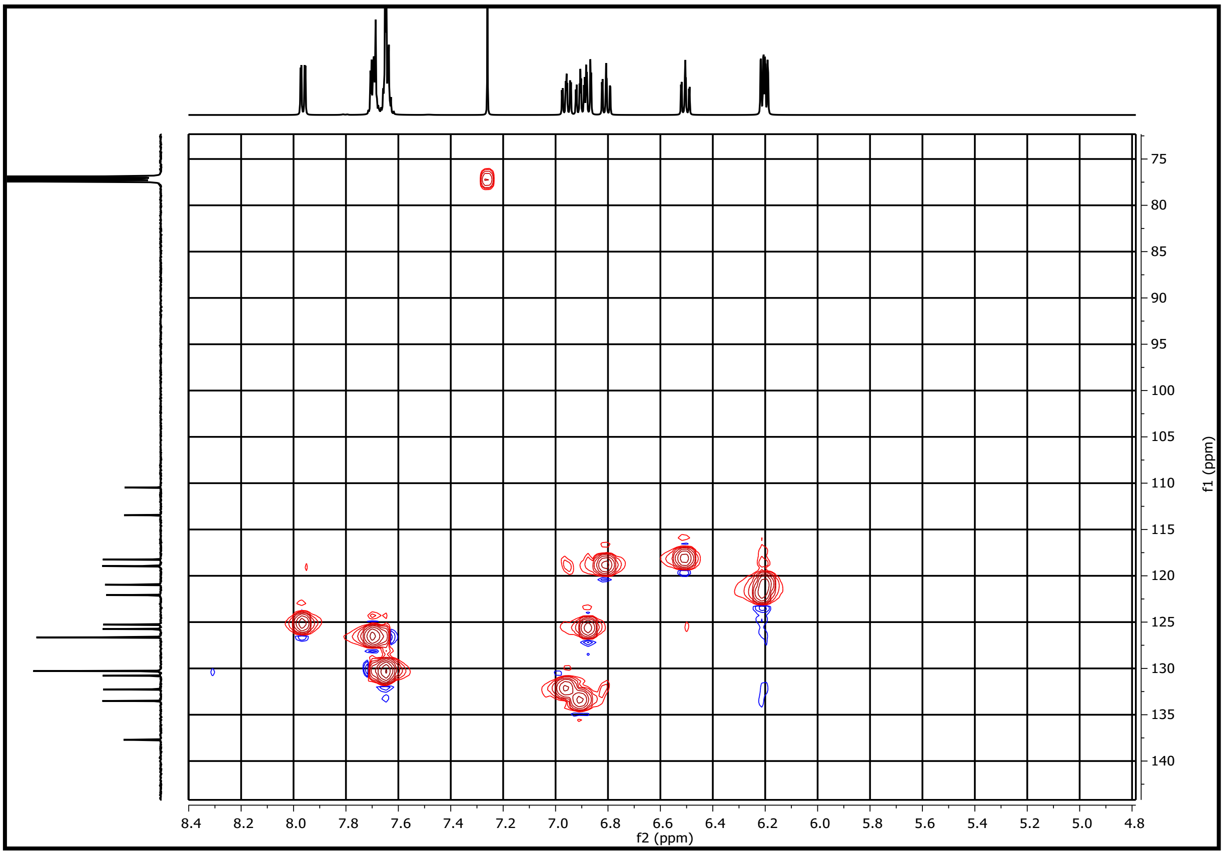

Figure S5. ^1H-^{13}C HSQC NMR spectrum of $Si(ONO)_2$ in $CDCl_3$

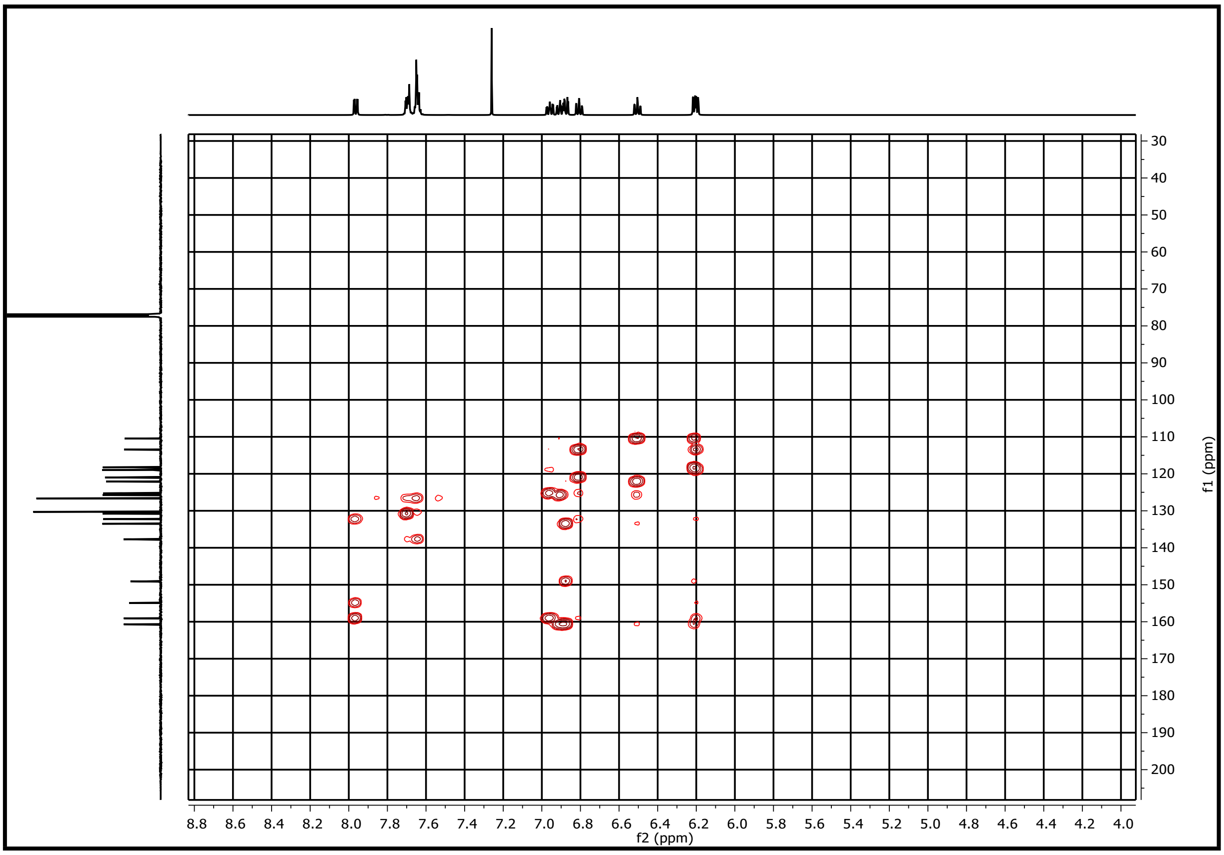

Figure S6. ^1H-^{13}C HMBC NMR spectrum of $Si(ONO)_2$ in $CDCl_3$

Supplementary figures and tables

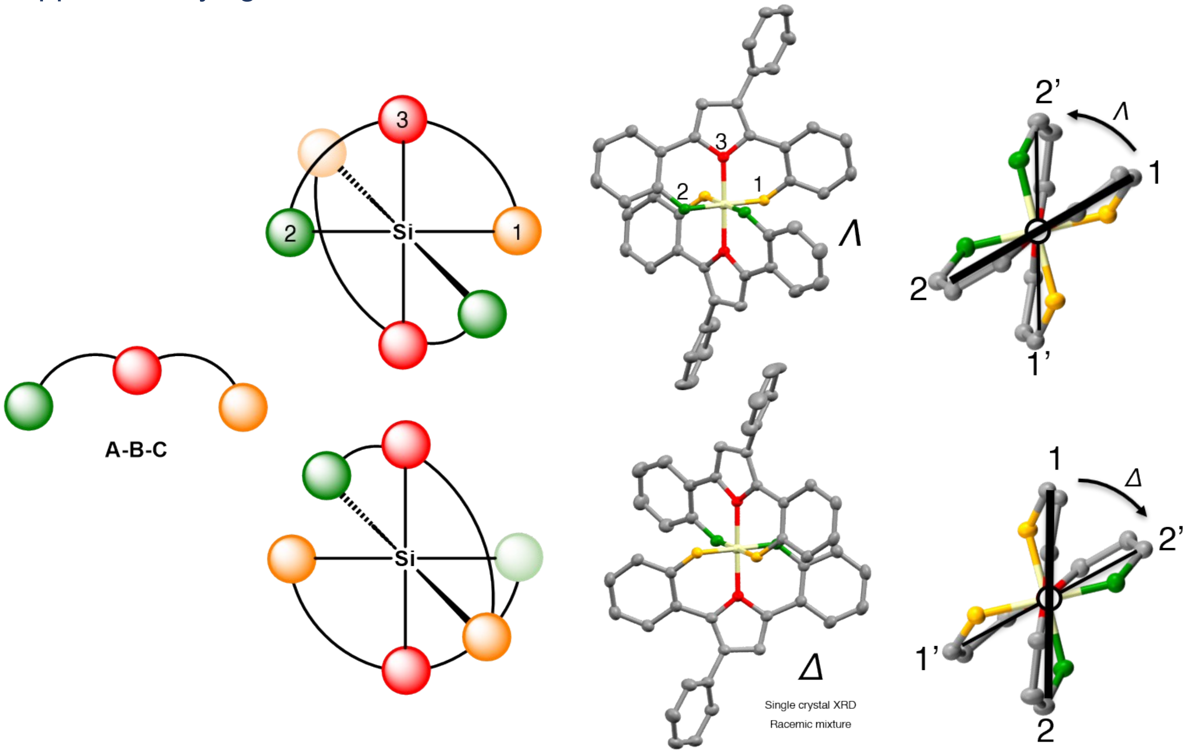

Figure S 7 - Stereochemistry assignment of Δ and Λ enantiomers, where the atoms of the A-B-C style O^N^O tridentate ligand are numbered 1 to 3 according to Cahn-Ingold-Prelog (CIP) rules.

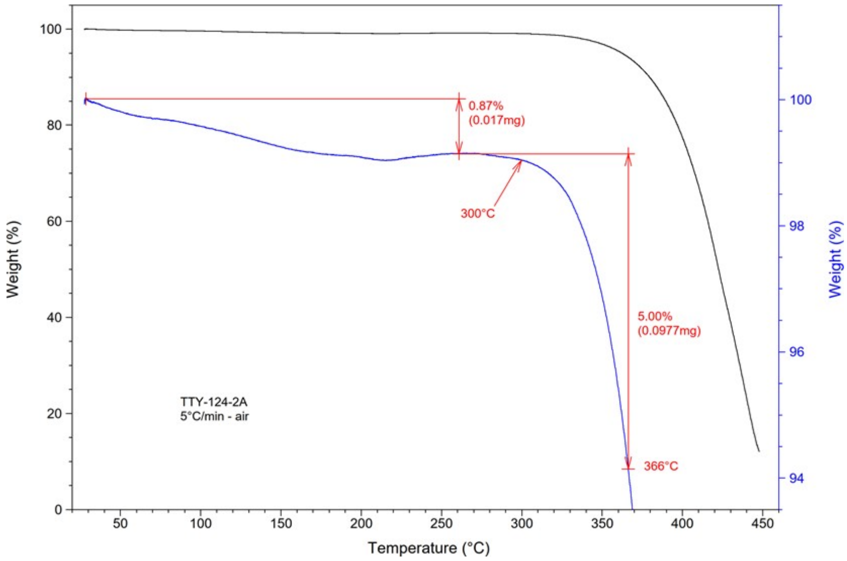

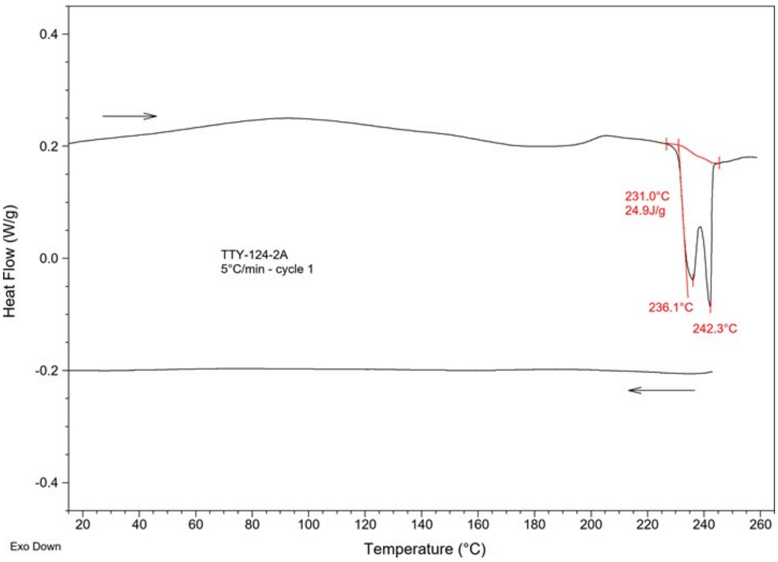

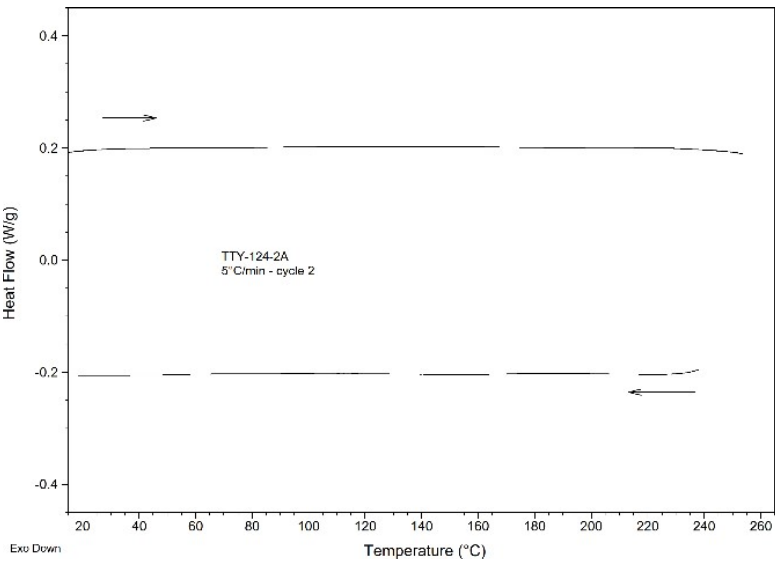

Figure S 8 - Crystal structure and TGA/DSC analysis for **Si(ONO)$_2$**, HPLC purified and recrystallized. TGA Q50 from TA instruments (5°C/min, air) (top). POM: Weight loss from degradation becomes significant above ca. 300°C. 5% weight loss temperature $T_{5\%}$ = 366°C. The slight weight loss below 170°C is related to the release of a small volatile fraction. DSC Q1000 from TA instruments (5°C/min endotherm up), cycle 1 (center) and cycle 2 (bottom). **Si(ONO)$_2$** is an amorphous solid that crystallizes on first heating at 230-240°C. No melting is observed on POM until 300°C. No phase change occurs on cooling and second heating.

Analytical chiral HPLC separation

The sample is dissolved in a mixture of ethanol, CH_2Cl_2 and heptane, injected on a Chiralpak IB N-5 chiral column, and detected with an UV detector at 290 nm and a circular dichroism detector at 254 nm. The flow-rate is 1 mL/min.

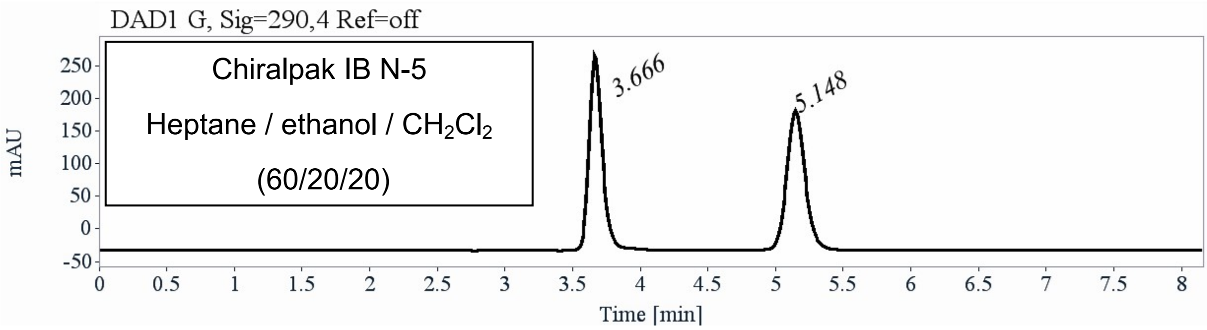

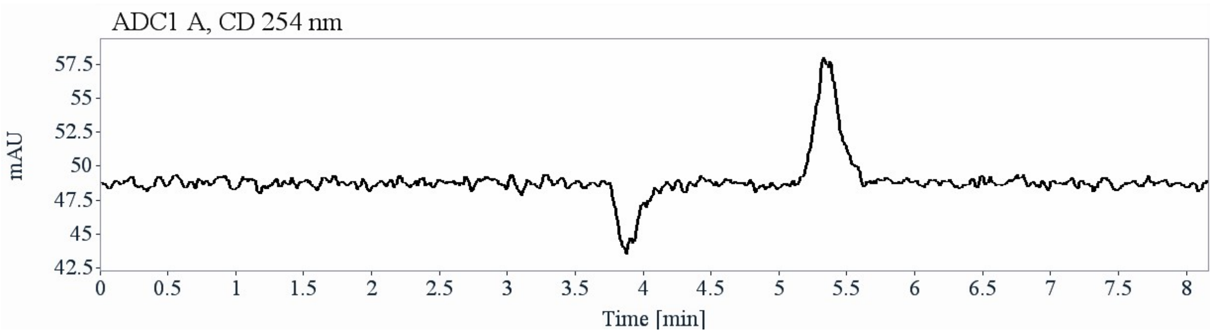

RT [min]	Area	Area%	Capacity Factor	Enantioselectivity	Resolution (USP)
3.67	2091	50.48	0.24		
5.15	2051	49.52	0.75	3.07	7.03
Sum	4142	100.00			

Preparative separation

Sample preparation: About 74 mg of compound $Si(ONO)_2$ are dissolved in 3 mL of a mixture of CH_2Cl_2 and hexane (50/50).

Chromatographic conditions: Chiralpak IB N-5 (250 x 10 mm), hexane / ethanol / CH_2Cl_2 (60/20/20) as mobile phase, flow-rate = 5 mL/min, UV detection at 290 nm.

Injections: 35 times 90 µL, every 5.4 minutes.

First fraction: 32 mg of the first eluted enantiomer with ee >99.5%

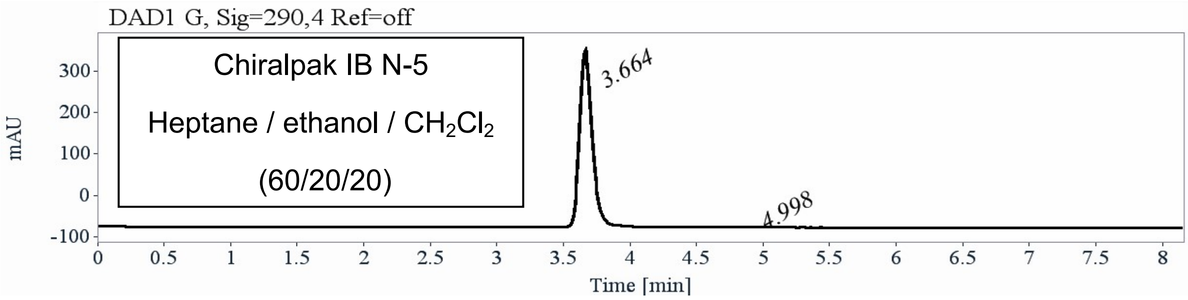

RT [min]	Area	Area%
3.66	2893	99.93
5.00	2	0.07
Sum	2895	100.00

Second fraction: 32 mg of the second eluted enantiomer with ee >99.5 %

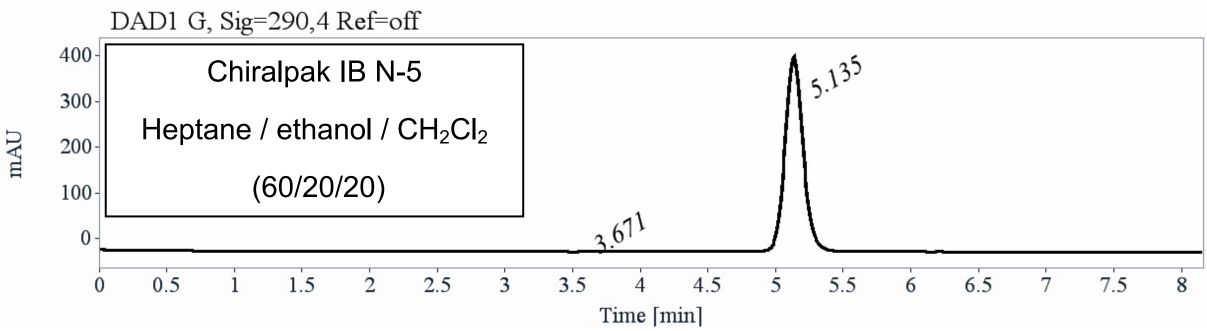

RT [min]	Area	Area%
3.67	5	0.12
5.14	4000	99.88
Sum	4004	100.00

Intermediate: 6 mg of racemate

Photophysical and chiroptical studies

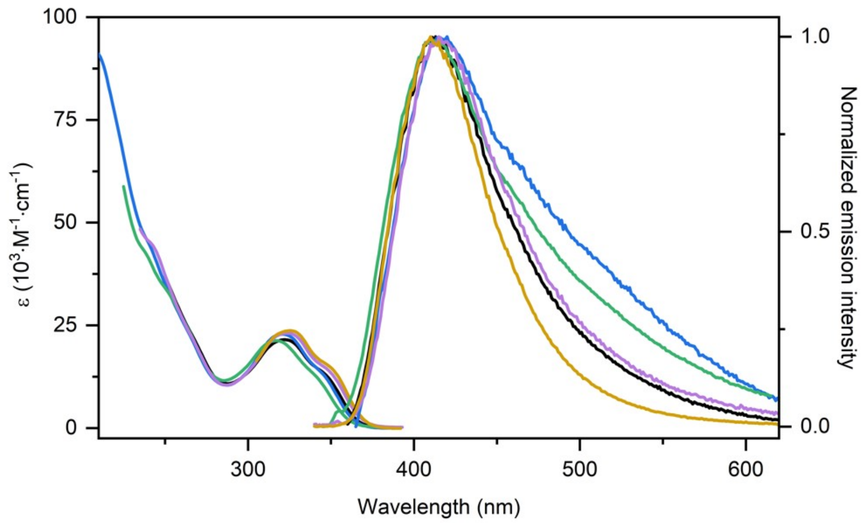

Figure S 9 - UV-vis absorption and photoluminescence emission in dilute solvents of increasing polarity (2×10^{-5} M) for $Si(ONO)_2$. Colour code: toluene (yellow), THF (pink), CH_2Cl_2 (black), CH_3CN (blue), MeOH (green). Emission spectra were recorded upon excitation at λ_{exc} = 320 nm.

Table S 1 - Photophysical properties of **$Si(ONO)_2$** and **$(ONO)H_2$** in dilute air-equilibrated organic solvents (2.0×10^{-5} M) at room temperature. Radiative and non-radiative rate constants were determined with the equations $k_r = PLQY/\tau$ and $k_{nr} = (1 - PLQY)/\tau$ respectively. *sh* denotes a shoulder. *br* denotes a broad signal.

compound	*solvent*	λ_{max} (ε) [nm, (10^3 M^{-1} cm^{-1})]	λ_{em} [nm]	PLQY (%)	τ_{obs} [ns]	$\bar{\tau}_{obs}$ [ns]	k_r [10^8 s^{-1}]	k_{nr} [10^8 s^{-1}]
$(ONO)H_2$	*CH_2Cl_2*	298*sh* (12.81), 308 (14.60)	519	1	2.49 (65%) 11.3 (35%)	8.76	0.01	1.13
$Si(ONO)_2$	*Toluene*	325 (23.72) 348 (15.36)	410	21	3.30	-	0.64	2.39
	THF	242*sh* (44.78) 324 (23.09) 349*sh* (13.86)	414	9	2.74	-	0.33	3.32
	CH_2Cl_2	322 (21.53) 345*sh* (13.61)	414	12	3.26	-	0.37	2.70
	CH_3CN	239*sh* (45.87) 322 (22.85) 346*sh* (12.75)	417	2	2.18 (13%) 0.77 (87%)	1.19	0.17	8.25
	MeOH	238*sh* (42.81) 251*sh* (33.55) 317 (21.27)	413	2	1.44 (29%) 0.87 (69%)	1.10	0.18	8.91

Table S 2 - Optical rotation values obtained for the two **$Si(ONO)_2$** enantiomers.

λ (nm)	Λ-**$Si(ONO)_2$** $[\alpha]_\lambda^{25}$ (1.6 g/mL in CH_2Cl_2)	Δ-**$Si(ONO)_2$** $[\alpha]_\lambda^{25}$ (1.6 g/mL in CH_2Cl_2)
589	+ 5	- 5
578	+ 5	- 5
546	+ 6	- 6
436	+ 8	- 8
405	+ 17	- 17

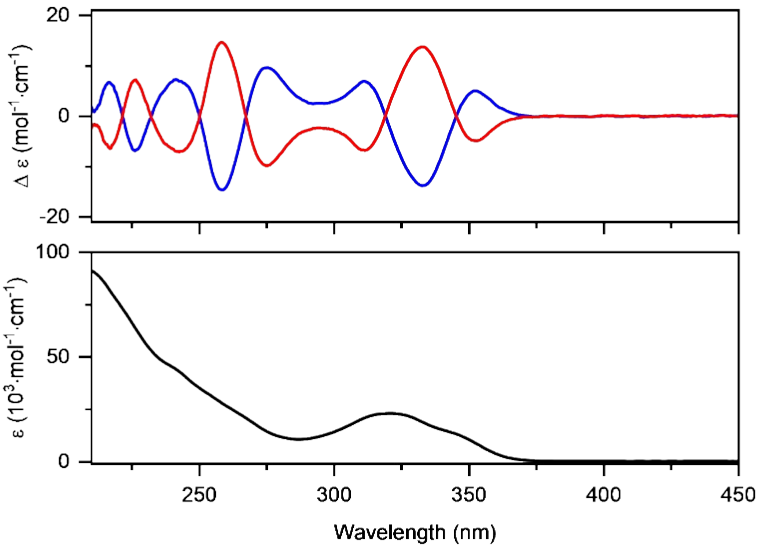

Figure S 10 - *Top*: experimental electronic circular dichroism spectra of **Λ-Si(O^{1}NO^2)$_2$** (first eluted, blue trace) and **Δ-Si(O^{1}NO^2)$_2$** (second eluted, red trace) in dilute CH_3CN at concentration of 2×10^{-4} M. *Bottom*: experimental UV-vis electronic absorption spectra of ***rac*-Si(O^{1}NO^2)$_2$** in dilute CH_3CN at concentration of 2×10^{-5} M.

Table S 3 - Experimental electronic circular dichroism data of the two **Si(O^{1}NO^2)$_2$** enantiomers in dilute CH_3CN (2×10^{-4} M).

Isomer	λ_{max} ($\Delta\varepsilon$) [nm, (M^{-1} cm^{-1})]
Λ	216 (6.73), 226 (-6.72), 241 (7.26), **259** (-14.68), 274 (9.55), 312 (6.77), 332 (-13.77), 351 (4.70)
Δ	216 (-6.46), 226 (7.15), 243 (-7.01), **258** (14.49), 275 (-9.84), 312 (-6.77), 332 (-13.56), 352 (-4.90)

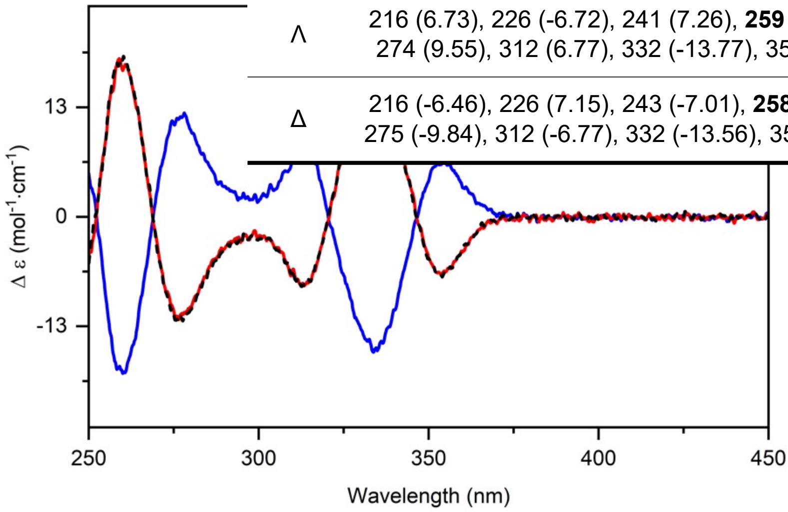

Figure S 11 - Electronic circular dichroism spectra in dilute CH_2Cl_2 (2×10^{-4} M) of the first eluted (blue trace), second eluted (red trace) and second diluted heat-treated (black dashed trace) enantiomer.

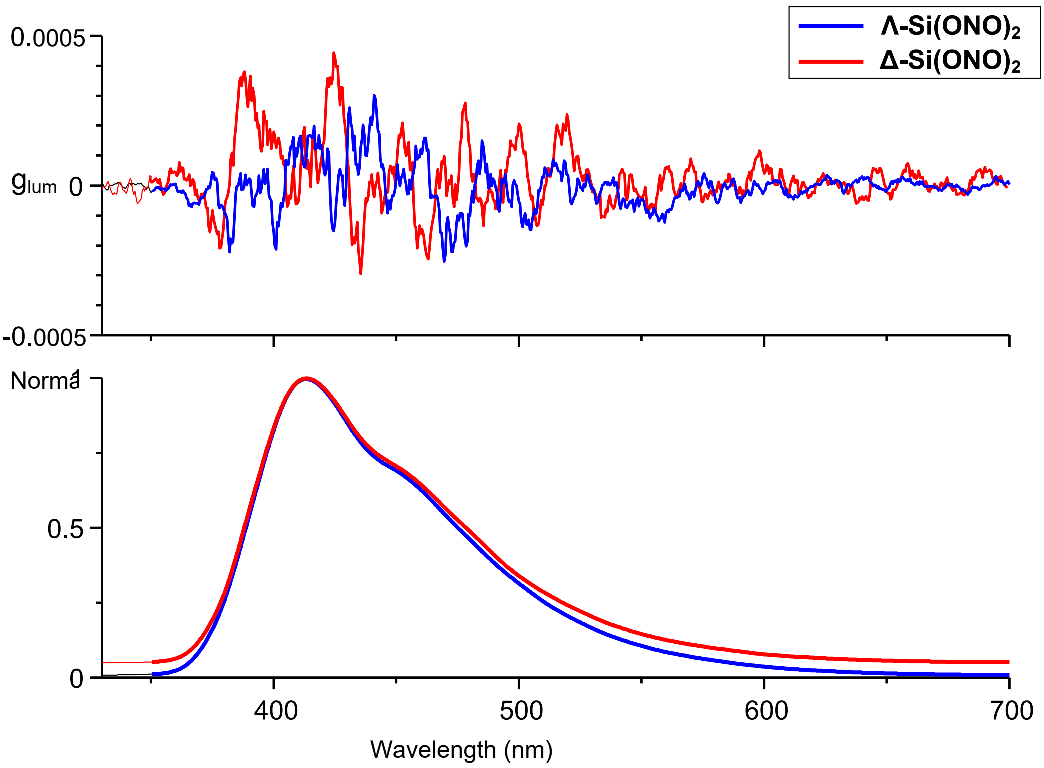

Figure S 12 - Circularly polarized luminescence spectra (*top*) and photoluminescence emission (*bottom*) of **Λ-Si(O[1]NO[2])$_2$** (first eluted, blue trace) and **Δ-Si(O[1]NO[2])$_2$** (second eluted, red trace) in dilute CH_2Cl_2 (1×10^{-5} M). Emission spectra were recorded upon excitation at λ_{exc} = 325 nm, with 9 accumulations. The two enantiomers of **Si(ONO)$_2$** show negligible CPL at λ_{em} = 400-450 nm with a $|g_{lum}|$ not higher than 5×10^{-4}.

Computational investigation

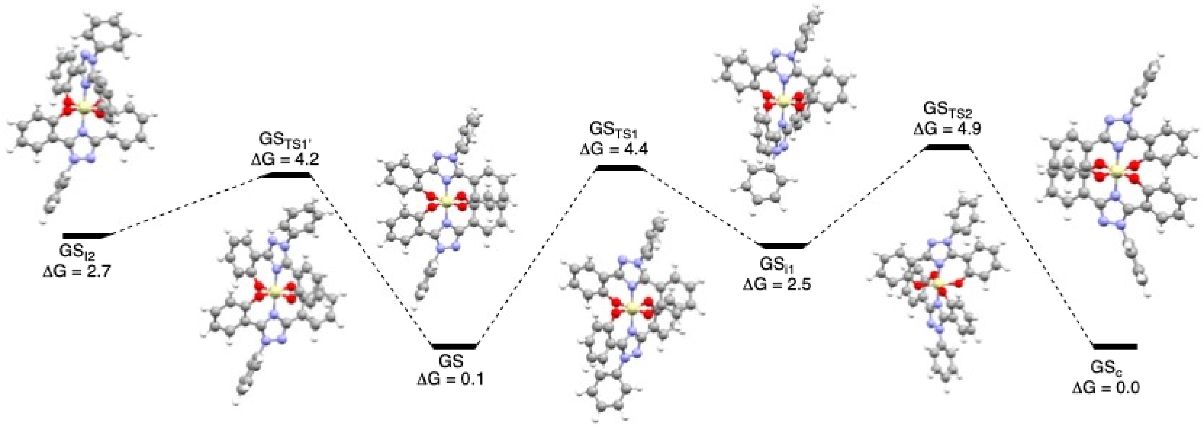

Figure S 13 - Computed interconversion path for the **Si(ONO)$_2$** complex. Gibbs free energies are given in kcal mol^{-1}.

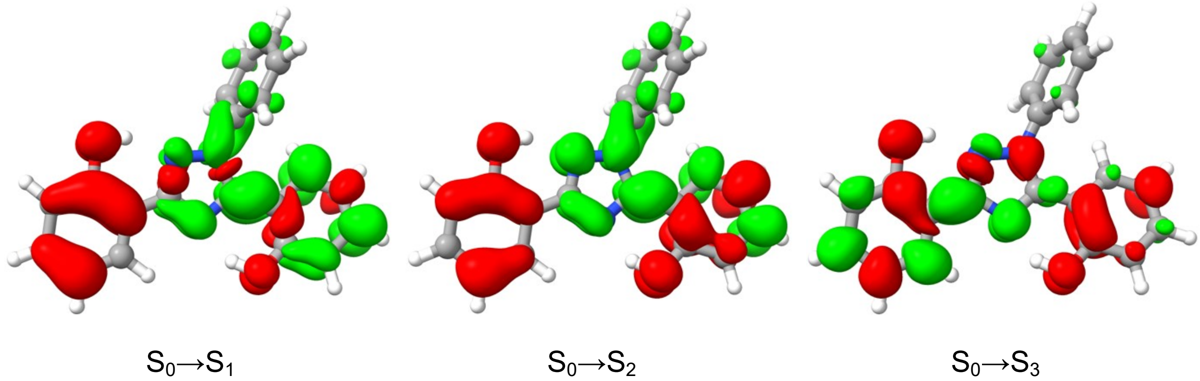

Figure S 14 - Electronic density difference maps (EDDMs) computed for $S_0 \rightarrow S_1$ (left), $S_0 \rightarrow S_2$ (center), and $S_0 \rightarrow S_3$ (right) at Franck–Condon geometry for **(ONO)H$_2$** ligand. Electronically enriched and depleted areas are colored in green and red, respectively.

Table S 4 - Computed electronic transition for the **(ONO)H$_2$** ligand.

State	E_{abs} (eV)	λ_{abs} (nm)	f_{osc}
S1	4.003	310	1.87E-01
S2	4.169	297	1.29E-01
S3	4.337	286	3.02E-01
S4	4.558	272	3.24E-02
S5	4.626	268	1.70E-03
S6	4.654	266	1.68E-02
S7	4.779	259	1.48E-02
S8	4.931	251	8.96E-02
S9	4.965	250	3.40E-01
S10	4.997	248	1.05E-01
S11	5.079	244	4.10E-03
S12	5.096	243	4.50E-03
S13	5.167	240	5.76E-02
S14	5.278	235	1.18E-02
S15	5.355	232	2.54E-02
S16	5.421	229	2.72E-02
S17	5.492	226	1.57E-02
S18	5.523	224	7.15E-02
S19	5.573	222	7.00E-03
S20	5.614	221	1.24E-01

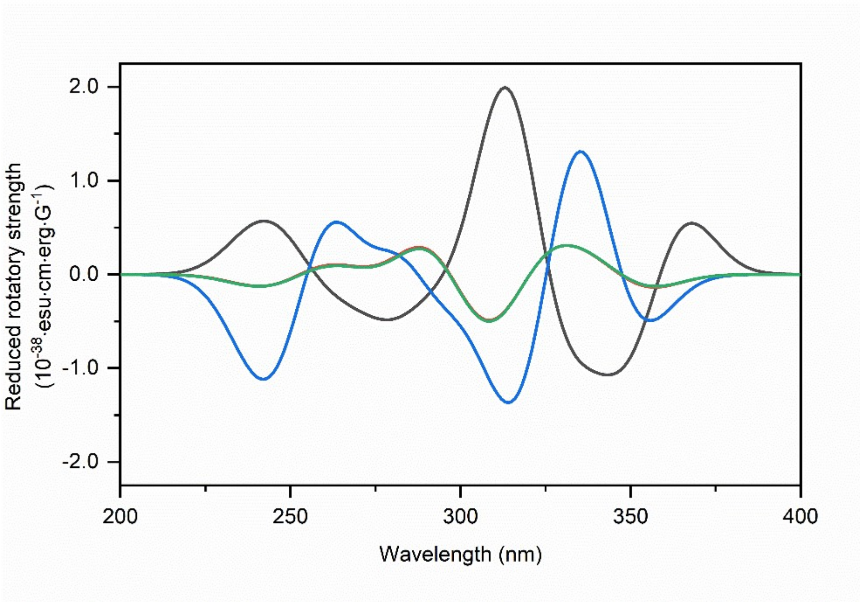

Figure S 15 - Computed ECD spectra of the different conformers of **$Si(ONO)_2$** complex. The configuration of GS_a is Λ(λ,λ) (black), GS_{i1} is Λ(λ,δ) (red), GS_{i2} is Λ(δ,λ) (green) and GS_b is Λ(δ,δ) (blue).

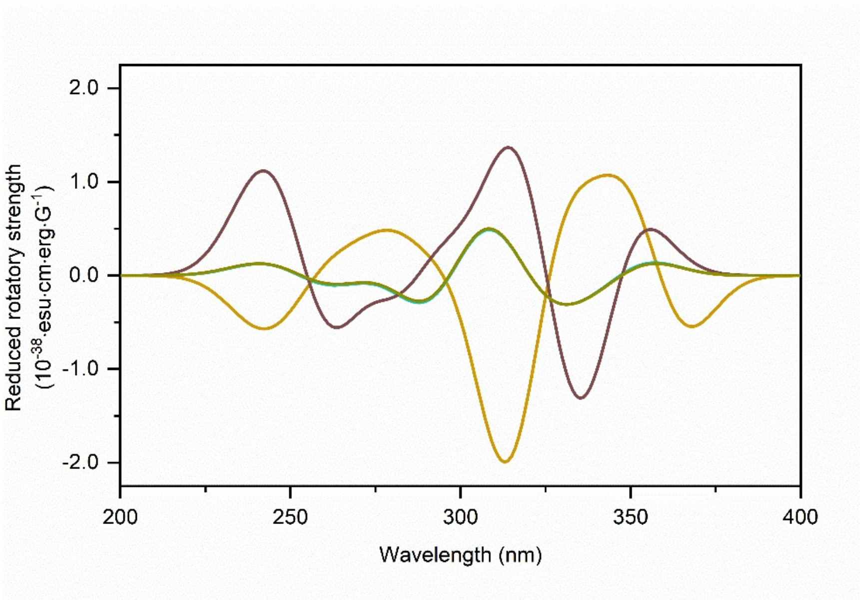

Figure S 16 - Computed ECD spectra of the different enantiomers of the conformers of **$Si(ONO)_2$** complex. The configuration of GS_a is Δ(δ,δ) (yellow), GS_{i1} is Δ(δ,λ) (teal), GS_{i2} is Δ(λ,δ) (dark green) and GS_b is Δ(λ,λ) (brown).

Table S 5 - Computed electronic transition for the GS_a and GS_b structures of **$Si(ONO)_2$** complex.

	GS_a $\Lambda(\lambda,\lambda)$					**GS_b $\Lambda(\delta,\delta)$**			
State	**E_{abs} (eV)**	**λ_{abs} (nm)**	**f_{osc}**	**R**		**E_{abs} (eV)**	**λ_{abs} (nm)**	**f_{osc}**	**R**
S1	3.429	362	2.06E-01	108.2		3.447	360	2.05E-01	-0.7
S2	3.530	351	6.50E-03	-136.0		3.544	350	2.01E-02	-79.9
S3	3.718	333	3.00E-04	-13.1		3.713	334	1.36E-02	203.9
S4	3.841	323	3.28E-02	-323.3		3.839	323	1.00E-03	8.3
S5	3.854	322	7.70E-03	37.2		3.873	320	1.45E-01	-267.1
S6	3.901	318	1.41E-01	407.5		3.891	319	1.36E-01	218.8
S7	3.953	314	1.35E-02	-114.5		3.943	314	3.38E-02	-145.8
S8	3.970	312	2.36E-01	140.9		3.951	314	6.87E-02	-13.3
S9	4.051	306	7.13E-02	20.3		3.995	310	1.00E-04	0.9
S10	4.128	300	1.25E-02	-74.4		4.114	301	8.07E-02	42.9
S11	4.265	291	1.17E-02	-83.0		4.289	289	2.64E-02	3.5
S12	4.275	290	1.30E-01	169.1		4.291	289	1.66E-01	-260.5
S13	4.327	287	7.28E-02	-30.1		4.324	287	3.87E-02	127.1
S14	4.364	284	1.00E-04	0.3		4.353	285	3.40E-03	2.4
S15	4.382	283	1.26E-01	126.8		4.356	285	1.10E-01	124.5
S16	4.388	283	5.62E-02	-239.0		4.365	284	2.90E-03	-2.7
S17	4.406	281	3.66E-02	37.5		4.407	281	4.14E-02	19.8
S18	4.455	278	3.00E-03	-11.8		4.445	279	2.31E-02	47.3
S19	4.480	277	1.90E-03	-12.0		4.495	276	3.36E-02	-23.9
S20	4.493	276	3.48E-02	24.2		4.500	276	9.24E-02	-85.7
S21	4.514	275	1.30E-03	-3.0		4.514	275	1.60E-03	-4.6
S22	4.532	274	4.49E-02	32.3		4.560	272	4.83E-02	-11.9
S23	4.541	273	1.30E-03	-2.9		4.588	270	3.50E-03	6.7
S24	4.592	270	2.59E-02	-29.4		4.607	269	4.70E-03	13.5
S25	4.723	263	3.00E-03	2.4		4.740	262	6.00E-04	-0.2
S26	4.724	262	6.10E-03	4.1		4.743	261	2.00E-03	-2.0
S27	4.783	259	2.80E-03	-11.5		4.782	259	4.10E-03	4.2
S28	4.793	259	6.40E-03	1.6		4.784	259	2.00E-04	0.6
S29	4.812	258	1.00E-04	0.4		4.806	258	3.85E-02	143.9
S30	4.830	257	4.29E-02	49.8		4.830	257	1.11E-01	15.8
S31	4.832	257	3.42E-02	-118.4		4.840	256	6.33E-02	70.0
S32	4.842	256	1.82E-01	22.3		4.856	255	8.62E-02	-22.0
S33	4.887	254	3.19E-02	-130.9		4.861	255	2.15E-02	17.8
S34	4.894	253	2.36E-01	191.1		4.871	255	3.58E-02	-69.5
S35	4.905	253	1.60E-03	-0.7		4.907	253	3.15E-02	25.5
S36	4.914	252	1.61E-02	-0.8		4.916	252	1.35E-01	-158.4
S37	4.974	249	2.13E-02	4.2		4.960	250	3.00E-04	2.9
S38	4.989	249	4.00E-04	-4.5		4.974	249	2.19E-02	-9.8
S39	4.997	248	1.80E-03	-16.8		4.987	249	7.90E-03	25.8
S40	5.006	248	1.70E-03	-1.5		5.000	248	9.00E-03	20.5
S41	5.007	248	1.00E-02	-5.1		5.004	248	1.30E-03	6.1
S42	5.010	247	1.90E-03	-2.7		5.008	248	3.60E-03	-11.0
S43	5.018	247	7.74E-02	9.7		5.010	247	1.00E-04	-0.9
S44	5.034	246	3.50E-03	-27.5		5.021	247	6.50E-03	12.4
S45	5.041	246	7.40E-03	21.1		5.027	247	7.00E-02	-49.1
S46	5.075	244	1.93E-02	24.5		5.045	246	3.69E-02	39.9
S47	5.085	244	6.00E-04	-6.0		5.094	243	9.70E-03	4.8
S48	5.110	243	5.67E-02	28.6		5.105	243	2.28E-02	-55.6
S49	5.113	243	2.69E-02	-49.3		5.127	242	5.56E-02	19.5
S50	5.123	242	3.63E-01	63.1		5.127	242	3.34E-01	-71.3

Table S 6 - Computed electronic transition for the GS_{i1} and GS_{i2} structures of **$Si(ONO)_2$** complex.

	GS_{i1} $\Lambda(\lambda,\delta)$					GS_{i2} $\Lambda(\delta,\lambda)$			
State	**E_{abs} (eV)**	**λ_{abs} (nm)**	**f_{osc}**	**R**		**E_{abs} (eV)**	**λ_{abs} (nm)**	**f_{osc}**	**R**
S1	3.545	350	2.76E-02	-131.6		3.542	350	2.27E-02	-128.3
S2	3.556	349	1.18E-01	122.6		3.552	349	1.24E-01	119.8
S3	3.779	328	8.43E-02	103.1		3.776	328	8.64E-02	111.5
S4	3.792	327	3.62E-02	-89.2		3.788	327	3.10E-02	-95.9
S5	3.844	323	7.55E-02	-185.9		3.842	323	6.94E-02	-404.3
S6	3.850	322	8.95E-02	226.0		3.845	322	9.74E-02	443.4
S7	3.948	314	5.90E-03	4.3		3.945	314	3.80E-03	-3.4
S8	3.951	314	5.30E-03	-27.1		3.949	314	7.80E-03	-20.2
S9	3.993	310	2.52E-01	125.5		3.992	311	2.69E-01	209.9
S10	3.996	310	7.79E-02	-173.6		3.994	310	6.17E-02	-258.2
S11	4.210	294	8.24E-02	-212.7		4.208	295	8.18E-02	-217.7
S12	4.227	293	1.52E-01	252.8		4.226	293	1.53E-01	258.6
S13	4.367	284	8.00E-04	-0.5		4.366	284	1.00E-03	-0.3
S14	4.374	283	1.94E-02	1.1		4.373	283	2.36E-02	-1.2
S15	4.387	283	2.15E-02	-15.7		4.386	283	2.14E-02	-15.0
S16	4.392	282	4.96E-02	-11.3		4.391	282	4.99E-02	-14.2
S17	4.419	281	2.66E-02	27.5		4.418	281	3.07E-02	26.3
S18	4.425	280	1.25E-02	-12.0		4.425	280	1.16E-02	-10.1
S19	4.448	279	2.57E-02	-23.3		4.446	279	2.65E-02	-28.7
S20	4.451	279	3.99E-02	17.5		4.450	279	3.24E-02	24.8
S21	4.514	275	5.00E-03	-2.2		4.512	275	5.00E-03	-4.5
S22	4.523	274	7.10E-03	6.8		4.518	274	6.70E-03	8.8
S23	4.538	273	1.87E-02	2.2		4.538	273	1.95E-02	2.2
S24	4.543	273	1.40E-03	-4.2		4.544	273	1.00E-03	-4.2
S25	4.664	266	5.20E-03	1.7		4.667	266	5.90E-03	2.6
S26	4.671	265	3.10E-03	-0.9		4.673	265	2.30E-03	-1.8
S27	4.755	261	1.20E-03	1.2		4.760	260	1.10E-03	2.7
S28	4.760	260	2.10E-03	-0.4		4.760	260	2.40E-03	-1.8
S29	4.775	260	1.05E-02	-23.1		4.776	260	1.08E-02	-20.4
S30	4.781	259	1.43E-02	27.4		4.783	259	1.53E-02	25.6
S31	4.851	256	5.62E-02	16.0		4.850	256	5.55E-02	-10.8
S32	4.856	255	5.06E-02	4.5		4.852	256	7.21E-02	28.5
S33	4.869	255	2.12E-01	221.7		4.868	255	2.02E-01	209.0
S34	4.873	254	1.99E-01	-227.3		4.872	254	1.88E-01	-213.5
S35	4.890	254	9.00E-04	2.1		4.894	253	2.70E-03	2.0
S36	4.897	253	5.40E-03	-0.7		4.899	253	5.00E-03	-4.7
S37	4.906	253	6.91E-02	40.0		4.904	253	6.65E-02	45.3
S38	4.907	253	4.71E-02	-60.4		4.906	253	4.72E-02	-62.6
S39	4.981	249	4.50E-03	4.5		4.980	249	5.00E-03	5.8
S40	4.988	249	1.96E-02	4.6		4.987	249	2.09E-02	3.8
S41	4.997	248	1.20E-03	1.2		4.996	248	2.20E-03	1.8
S42	5.003	248	8.70E-03	2.9		5.003	248	9.70E-03	3.2
S43	5.011	247	5.10E-03	1.2		5.009	248	8.70E-03	-2.7
S44	5.014	247	7.20E-03	-6.5		5.013	247	1.00E-03	-3.4
S45	5.027	247	2.30E-03	1.7		5.024	247	2.90E-03	5.9
S46	5.030	246	2.20E-03	0.7		5.026	247	1.80E-03	-3.1
S47	5.075	244	1.61E-02	-60.7		5.073	244	1.57E-02	-62.1
S48	5.086	244	1.93E-02	70.0		5.085	244	2.21E-02	73.0
S49	5.145	241	6.42E-02	-38.5		5.145	241	6.62E-02	-39.6
S50	5.174	240	8.54E-02	14.8		5.173	240	8.73E-02	13.8

Table S 7 - Computed electronic transition for Delta GS_a and Delta GS_b structures of **$Si(ONO)_2$** complex.

	GS_a $\Delta(\delta,\delta)$					GS_b $\Delta(\lambda,\lambda)$			
State	E_{abs} (eV)	λ_{abs} (nm)	f_{osc}	R		E_{abs} (eV)	λ_{abs} (nm)	f_{osc}	R
S1	3.429	362	2.06E-01	-108.2		3.447	360	2.05E-01	0.7
S2	3.530	351	6.50E-03	136.0		3.544	350	2.01E-02	79.9
S3	3.718	333	3.00E-04	13.1		3.713	334	1.36E-02	-203.9
S4	3.841	323	3.28E-02	323.3		3.839	323	1.00E-03	-8.3
S5	3.854	322	7.70E-03	-37.2		3.873	320	1.45E-01	267.1
S6	3.901	318	1.41E-01	-407.5		3.891	319	1.36E-01	-218.8
S7	3.953	314	1.35E-02	114.5		3.943	314	3.38E-02	145.8
S8	3.970	312	2.36E-01	-140.9		3.951	314	6.87E-02	13.3
S9	4.051	306	7.13E-02	-20.3		3.995	310	1.00E-04	-0.9
S10	4.128	300	1.25E-02	74.4		4.114	301	8.07E-02	-42.9
S11	4.265	291	1.17E-02	83.0		4.289	289	2.64E-02	-3.5
S12	4.275	290	1.30E-01	-169.1		4.291	289	1.66E-01	260.5
S13	4.327	287	7.28E-02	30.1		4.324	287	3.87E-02	-127.1
S14	4.364	284	1.00E-04	-0.3		4.353	285	3.40E-03	-2.4
S15	4.382	283	1.26E-01	-126.8		4.356	285	1.10E-01	-124.5
S16	4.388	283	5.62E-02	239.0		4.365	284	2.90E-03	2.7
S17	4.406	281	3.66E-02	-37.5		4.407	281	4.14E-02	-19.8
S18	4.455	278	3.00E-03	11.8		4.445	279	2.31E-02	-47.3
S19	4.480	277	1.90E-03	12.0		4.495	276	3.36E-02	23.9
S20	4.493	276	3.48E-02	-24.2		4.500	276	9.24E-02	85.7
S21	4.514	275	1.30E-03	3.0		4.514	275	1.60E-03	4.6
S22	4.532	274	4.49E-02	-32.3		4.560	272	4.83E-02	11.9
S23	4.541	273	1.30E-03	2.9		4.588	270	3.50E-03	-6.7
S24	4.592	270	2.59E-02	29.4		4.607	269	4.70E-03	-13.5
S25	4.723	263	3.00E-03	-2.4		4.740	262	6.00E-04	0.2
S26	4.724	262	6.10E-03	-4.1		4.743	261	2.00E-03	2.0
S27	4.783	259	2.80E-03	11.5		4.782	259	4.10E-03	-4.2
S28	4.793	259	6.40E-03	-1.6		4.784	259	2.00E-04	-0.6
S29	4.812	258	1.00E-04	-0.4		4.806	258	3.85E-02	-143.9
S30	4.830	257	4.29E-02	-49.8		4.830	257	1.11E-01	-15.8
S31	4.832	257	3.42E-02	118.4		4.840	256	6.33E-02	-70.0
S32	4.842	256	1.82E-01	-22.3		4.856	255	8.62E-02	22.0
S33	4.887	254	3.19E-02	130.9		4.861	255	2.15E-02	-17.8
S34	4.894	253	2.36E-01	-191.1		4.871	255	3.58E-02	69.5
S35	4.905	253	1.60E-03	0.7		4.907	253	3.15E-02	-25.5
S36	4.914	252	1.61E-02	0.8		4.916	252	1.35E-01	158.4
S37	4.974	249	2.13E-02	-4.2		4.960	250	3.00E-04	-2.9
S38	4.989	249	4.00E-04	4.5		4.974	249	2.19E-02	9.8
S39	4.997	248	1.80E-03	16.8		4.987	249	7.90E-03	-25.8
S40	5.006	248	1.70E-03	1.5		5.000	248	9.00E-03	-20.5
S41	5.007	248	1.00E-02	5.1		5.004	248	1.30E-03	-6.1
S42	5.010	247	1.90E-03	2.7		5.008	248	3.60E-03	11.0
S43	5.018	247	7.74E-02	-9.7		5.010	247	1.00E-04	0.9
S44	5.034	246	3.50E-03	27.5		5.021	247	6.50E-03	-12.4
S45	5.041	246	7.40E-03	-21.1		5.027	247	7.00E-02	49.1
S46	5.075	244	1.93E-02	-24.5		5.045	246	3.69E-02	-39.9
S47	5.085	244	6.00E-04	6.0		5.094	243	9.70E-03	-4.8
S48	5.110	243	5.67E-02	-28.6		5.105	243	2.28E-02	55.6
S49	5.113	243	2.69E-02	49.3		5.127	242	5.56E-02	-19.5
S50	5.123	242	3.63E-01	-63.1		5.127	242	3.34E-01	71.3

Table S 8 - Computed electronic transition for Delta GS_{i1} and Delta GS_{i2} structures of **Si(ONO)$_2$** complex.

	GS_{i1} $\Delta(\delta,\lambda)$					GS_{i2} $\Delta(\lambda,\delta)$			
State	E_{abs} (eV)	λ_{abs} (nm)	f_{osc}	R		E_{abs} (eV)	λ_{abs} (nm)	f_{osc}	R
S1	3.545	350	2.76E-02	131.6		3.542	350	2.27E-02	128.3
S2	3.556	349	1.18E-01	-122.6		3.552	349	1.24E-01	-119.8
S3	3.779	328	8.43E-02	-103.1		3.776	328	8.64E-02	-111.5
S4	3.792	327	3.62E-02	89.2		3.788	327	3.10E-02	95.9
S5	3.844	323	7.55E-02	185.9		3.842	323	6.94E-02	404.3
S6	3.850	322	8.95E-02	-226.0		3.845	322	9.74E-02	-443.4
S7	3.948	314	5.90E-03	-4.3		3.945	314	3.80E-03	3.4
S8	3.951	314	5.30E-03	27.1		3.949	314	7.80E-03	20.2
S9	3.993	310	2.52E-01	-125.5		3.992	311	2.69E-01	-209.9
S10	3.996	310	7.79E-02	173.6		3.994	310	6.17E-02	258.2
S11	4.210	294	8.24E-02	212.7		4.208	295	8.18E-02	217.7
S12	4.227	293	1.52E-01	-252.8		4.226	293	1.53E-01	-258.6
S13	4.367	284	8.00E-04	0.5		4.366	284	1.00E-03	0.3
S14	4.374	283	1.94E-02	-1.1		4.373	283	2.36E-02	1.2
S15	4.387	283	2.15E-02	15.7		4.386	283	2.14E-02	15.0
S16	4.392	282	4.96E-02	11.3		4.391	282	4.99E-02	14.2
S17	4.419	281	2.66E-02	-27.5		4.418	281	3.07E-02	-26.3
S18	4.425	280	1.25E-02	12.0		4.425	280	1.16E-02	10.1
S19	4.448	279	2.57E-02	23.3		4.446	279	2.65E-02	28.7
S20	4.451	279	3.99E-02	-17.5		4.450	279	3.24E-02	-24.8
S21	4.514	275	5.00E-03	2.2		4.512	275	5.00E-03	4.5
S22	4.523	274	7.10E-03	-6.8		4.518	274	6.70E-03	-8.8
S23	4.538	273	1.87E-02	-2.2		4.538	273	1.95E-02	-2.2
S24	4.543	273	1.40E-03	4.2		4.544	273	1.00E-03	4.2
S25	4.664	266	5.20E-03	-1.7		4.667	266	5.90E-03	-2.6
S26	4.671	265	3.10E-03	0.9		4.673	265	2.30E-03	1.8
S27	4.755	261	1.20E-03	-1.2		4.760	260	1.10E-03	-2.7
S28	4.760	260	2.10E-03	0.4		4.760	260	2.40E-03	1.8
S29	4.775	260	1.05E-02	23.1		4.776	260	1.08E-02	20.4
S30	4.781	259	1.43E-02	-27.4		4.783	259	1.53E-02	-25.6
S31	4.851	256	5.62E-02	-16.0		4.850	256	5.55E-02	10.8
S32	4.856	255	5.06E-02	-4.5		4.852	256	7.21E-02	-28.5
S33	4.869	255	2.12E-01	-221.7		4.868	255	2.02E-01	-209.0
S34	4.873	254	1.99E-01	227.3		4.872	254	1.88E-01	213.5
S35	4.890	254	9.00E-04	-2.1		4.894	253	2.70E-03	-2.0
S36	4.897	253	5.40E-03	0.7		4.899	253	5.00E-03	4.7
S37	4.906	253	6.91E-02	-40.0		4.904	253	6.65E-02	-45.3
S38	4.907	253	4.71E-02	60.4		4.906	253	4.72E-02	62.6
S39	4.981	249	4.50E-03	-4.5		4.980	249	5.00E-03	-5.8
S40	4.988	249	1.96E-02	-4.6		4.987	249	2.09E-02	-3.8
S41	4.997	248	1.20E-03	-1.2		4.996	248	2.20E-03	-1.8
S42	5.003	248	8.70E-03	-2.9		5.003	248	9.70E-03	-3.2
S43	5.011	247	5.10E-03	-1.2		5.009	248	8.70E-03	2.7
S44	5.014	247	7.20E-03	6.5		5.013	247	1.00E-03	3.4
S45	5.027	247	2.30E-03	-1.7		5.024	247	2.90E-03	-5.9
S46	5.030	246	2.20E-03	-0.7		5.026	247	1.80E-03	3.1
S47	5.075	244	1.61E-02	60.7		5.073	244	1.57E-02	62.1
S48	5.086	244	1.93E-02	-70.0		5.085	244	2.21E-02	-73.0
S49	5.145	241	6.42E-02	38.5		5.145	241	6.62E-02	39.6
S50	5.174	240	8.54E-02	-14.8		5.173	240	8.73E-02	-13.8